International Journal of Current Engineering and Technology
E-ISSN 2277 – 4106, P-ISSN 2347 – 5161
©2023 INPRESSCO®, All Rights Reserved
Available at http://inpressco.com/category/ijcet

*Research Article*

# Partial Face Recognition using Robust Point Set Method

**Dr S Suryanarayana[1]and V Sundara Siva Kumar[2*]**

[1,2]Department of Electronics and Communication Engineering, Maturi Venkata Subba Rao (MVSR) Engineering College (Autonomous) Hyderabad, India

Received 25 March2023, Accepted 10 April2023, Available online13 April2023, **Vol.13, No.2 (March/April2023)**

***Abstract***

*This electronic document is a "live" template and already defines the components of your paper [title, text, heads, etc.] in its style sheet. Over the past three decades, a number of face recognition methods have been proposed in computer vision, and most of them use holistic face images for person identification. In many real-world scenarios especially some unconstrained environments, human faces might be occluded by other objects, and it is difficult to obtain fully holistic face images for recognition. To address this, we propose a new partial face recognition approach to recognize persons of interest from their partial faces. Given a pair of gallery image and probe face patch, we first detect key points and extract their local textural features. Then, we propose a robust point set matching method to discriminatively match these two extracted local feature sets, where both the textural information and geometrical information of local features are explicitly used for matching simultaneously. Finally, the similarity of two faces is converted as the distance between these two aligned feature sets. Experimental results on four public faces.*

***Keywords:*** *Insert face recognition, Robust point and Partial image.*

## 1. Introduction

### A. Baseline Algorithms

The proposed algorithm recognizes partial faces directly without manual face alignment; hence the approaches we selected for comparison should have the same capacity. In this spirit, we selected two approaches for comparison, which were our previous approach MLERPM and Liao et al.'s MKD-SRC-GTP.

Furthermore, we designed two new partial face recognition approaches for comparison. The first one was based on Li et al.'s work. We simply termed this new approach as Locally Affine Invariant Robust Point set Matching (LAIRPM). In terms of feature extraction, LAIRPM used the same features as ours, i.e. Sift Surf SILBP. After feature extraction, these extracted features were matched by Li's matching approach's is a matrix recording the local structure of the probe feature set, and it's derived by reconstructing each feature point with its local neighborhood. Neighborhood is built either through Delaunay Triangulation (DT) or k-nearest neighbor (kNN). We tried both schemes and found Knn with k = 5 achieved the best result. In terms of λ1 and λ2, LAIRPM utilized the same setting as in our RPSM (detailed in Section IV-C), where λ1 = 0.01 and λ2 = max(C). After feature matching, we define the matching distance metric dL for LAIRPM.

*Corresponding author's ORCID ID: 0000-0003-3533-0125
DOI: https://doi.org/10.14741/ijcet/v.13.2.9

The second approach was built upon CPD. We directly utilized its released code to match feature sets by geometric information. The non-rigid RBF kernel was employed for matching. In terms of the matching distance, it was simply set as the average Euclidean distance between the matched feature points. In the following experiments, unless specified, all methods including CPD, LAIRPM and MLERPM utilized Sift Surf SILBP as their local features.

### B. Evaluation of the Point-Set Distance Metric

To evaluate the proposed point-set distance metric $d_R$, we designed the following four baselines:

- *Geometry metric $d_G$:* This metric only considers geometric information in calculation, which is defined as

$$d_G = \frac{\lambda_1 \sum_{i,j} M ||f(l_i^p) - l_j^G||_1 + \lambda_3 ||Q\Phi||_1}{\left(\sum_{i,j} M_{i,j}\right)^2} \quad (1)$$

- *Textural metric $d_T$:* This metric only considers geometric information in calculation, which is defined as

$$d_T = \left(\sum_{i,j} M_{i,j} C_{i,j}\right) / \left(\sum_{i,j} M_{i,j}\right)^2 (2)$$

- *Affine transformation metric$d_A$:* This metric disregards the non-affine portion, which is defined as

$$d_A = \left(\sum_{i,j} M_{i,j}\lambda_1 ||f(l_i^p) - l_j^G||C_{ij}\right)/\left(\sum_{i,j} M_{i,j}\right)^2 \quad (3)$$

### C. Evaluation of the Point-Set Matching Performance

Note that RPSM aligns two matching images by deriving a non-linear geometric transformation function f(l). The transformation function f(l) minimizes the geometric distribution differences between their corresponding point sets. Hence, evaluation of RPSM's point set matching performance is equivalent to investigate whether f(l) can faithfully recover the ground-truth transformation between these two images. However, it's non-trivial to directly measure the accuracy of f(l), instead, we evaluated it through measuring RPSM's face alignment accuracy.

We compared RPSM with three state-of-the-art feature set matching approaches, namely CPD, GMM reg and MLERPM, as well as two recent facial landmark detection approaches which are CFAN and SDM. The release codes of these approaches were directly employed for alignment. Note that LAIRPM was not compared as it doesn't yield geometric transformation function. For a face pair, let's denote the ith landmark position of the holistic facial image as lHi , and the one of the partial face as lPi . Given the face pair and lH the feature set matching approach is able to derive a transformation function f (l), with which we can estimate the landmark positions of the partial face by f (lH ).

where di is the inter-pupil distance of the ith partial face, N is the number of landmarks (in this case N = 51), and error is the Normalized Root Mean Squared Error (NRMSE), which is defined as the average alignment error normalized by the inter-pupil distance. If the feature set matching approach can correctly uncover the transformation between the matching face pair, the Landmark detection error shall be small. For SDM and CFAN, their alignment accuracy was assessed by

$$\in = \frac{1}{N}\sum_{i=1} ||l_i^p - \hat{l}_i^p||^2/d_i \quad (4)$$

where l^P are their estimated landmark positions. Finally, the Cumulative Error Distribution (CED) curves of NRMSE were used to quantitatively evaluate the performance. Figure 1 show the CED curves results. Feature set matching approaches achieve significantly higher alignment accuracy than SDM and CFAN. This is because partial faces are extremely challenging for face alignment methods, where some key facial components (such as brows, mouth) can be missing. On the contrary, feature set matching approaches conduct face alignment by matching two local feature sets. It doesn't matter if any of the facial components are occluded or missing, so long as there exist similar facial patches between the matching faces. CED curves of various methods on 600 partial faces. Within the feature set matching group, our RPSM achieves the best performance. This is due to the fact that RPSM considers both the geometric consistency and textural similarity during alignment, while CPD and GMM reg only utilize the geometric information. In terms of MLERPM, it performs poorer than RPSM as its affine-part matching is unregulated, which may result in tilted and sheared facial images.

## 2. Partial Face Recognition Performance

### A. Partial Face Verification on LFW

We conducted face verification on LFW dataset, where we applied our algorithm on the original unaligned LFW images directly. We first used the Open CV implementation of the Viola-Jones face detector to detect and crop out the facial regions of all images. The cropped faces underwent the same random transformation process as in Section IV-E. Some sample partial face image pairs were shown in Fig. 5.2 Note that in this experiment, both the gallery and probe images were partial faces. In terms of the verification process, we strictly followed the experiment protocol in View 2 outlined on the homepage of LFW dataset. To demonstrate the effectiveness of our Sift Surf SILBP features, we added a group of experiments where comparing algorithms worked on Sift Surf features, denoted with postfix "-Sift Surf". First, we utilized CFAN to detect 25 inner facial landmarks for each image. Subsequently, each image was normalized to the frontal pose and was further resized to 5 scales. For each scale, fixed size image patches at all facial landmarks were cropped, which were then described by LBP features. Finally these LBP descriptors were concatenated to a 118, 000 dimensional feature. This feature was projected by PCA to 750 dimensions.

Columns in the red box: matched image pairs. Columns in the blue box: mismatched image pairs. For verification, Joint Bayesian was employed. We tested our implementation on the funneled LFW images with the unrestricted setting without outside training data, and it achieved 93.45% accuracy, which was comparable to the reported result (93.18%). To apply HDLBP in this partial face recognition scenario, we first employed CFAN to detect landmarks from the randomly transformed LFW images. The distance between the matched/mismatched image pairs were then calculated by applying the trained joint Bayesian model.

**Fig: 1** Example face images from the LFW dataset after random transformation in view 2.

The mean values of false positive rate and true positive rate corresponding to various thresholds formed the ROC curves for evaluation. The ROC curves of comparing algorithms are used and their classification accuracy (u) as well as their corresponding standard deviation (SE) .The result shows that RPSM working on Sift Surf SILBP achieves the highest classification accuracy.

Moreover, algorithms using Sift Surf SILBP have better performance than their counterparts on Sift Surf features, which show that SILBP can extract complementary information for Sift Surf features, benefiting the following feature matching process. HDLBP performs the poorest among the comparing approaches and its partial face recognition accuracy 49.32% significantly worse than its holistic face recognition accuracy 93.45%. The performance degradation is mainly due to the inefficiency of CFAN in dealing with partial faces. To our best knowledge, the state-of-the-art landmark detection approaches are unable to estimate facial landmarks robustly from partial faces, especially when one or more facial components are cropped out.

### B. Face Verification on Pub Fig

To further validate the effectiveness of our approach on face verification, we conducted face verification experiment on the selected PubFig dataset. To begin with, we constructed genuine matching pairs as well as imposter matching pairs. For genuine matches, we paired up every two of the five images for each identity; hence we had 1400 genuine matches. For imposter pairs, we randomly paired up two images from two identities to construct 1400 impostor matches for verification. The ROC curves were depicted in fig 5.4 and the accuracy (u) as well as its standard deviation (SE) .

From the ROC curves and classification accuracy, we find that our approach RPSM Sift Surf SILBP achieved the best verification performance, showing the efficacy of our approach. And algorithms working on Sift Surf SILBP features had better performance than its counterpart on Sift Surf features.

### C. Face Verification on Pub Fig

To demonstrate the strength of our algorithm on recognizing arbitrary partial face patches, we randomly transformed the images of the selected Pub Fig dataset (evaluation set) to generate partial face patches. The randomization process is as the same as the one detailed in Experiment IV-E. Some sample partial face images were shown on the bottom row in Fig.5.5.

With partial faces at hand, we randomly split this transformed dataset into five subsets, where each subset had 140 images with one image per person, and any two subsets didn't share the same images. For testing, we conducted five-fold testing scheme: within each round, one subset was selected as gallery images, and the rest four as probe images. Therefore, in this experiment, both the gallery and probe images were partial faces, which posed great challenge to recognition approaches. To demonstrate the effectiveness of our matching approach, we added three baseline methods in addition to LAIRPM, MKD-SRC-GTP and MLERPM. These three baseline algorithms worked on textural part of local features (Sift 0Surf SILBP) alone.

- The first one was using Lowe's matching method to match textural feature sets of gallery images and probe images; the number of matching pairs was set as similarity criterion.
- The second one was Hausdorff distance (HausDist) which calculates the largest distance between closures of two textural feature sets.
- The third method was Earth Mover's Distance (EMD), which measures the minimum cost of transforming one distribution of textural feature set into the other, where we set number of K-means clusters to 8, which was the best result achieved across various values of k, ranging from 5 to 13.

1. Our method RPSM obtained the best recognition rates at most ranks. Note that it performed consistently better than MLERPM at all ranks, showing the benefits of regulating the affine transformation matrix.
2. LAIRPM and MKD-SRC-GTP had competitive performances against RPSM at large ranks, i. e., from Rank 15 onwards, yet their performances were poorer than RPSM's at the first 10 ranks, and higher recognition rates at these ranks are critical in practical applications.
3. HausDist, EMD and Lowe's matching approaches achieved poor performance. This is because matching only on texture features merely exploits partial information of face images, and texture features alone are not discriminative enough.

### D. Partial Face Identification under Occlusions

We conducted several partial face recognition under occlusion experiments on AR database as well as on EYB database. For fair comparison with existing holistic methods, all these probe images and gallery images were cropped to 128 × 128 pixels and properly aligned.

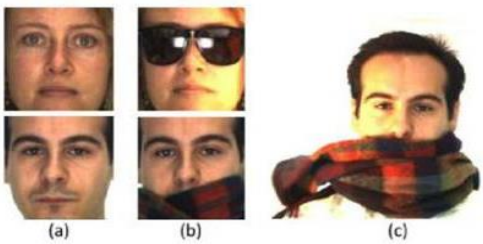


**Fig: 2** Samples from the AR dataset. (a) Cropped gallery image with neutral expression. (b) Cropped probe images occluded by sunglasses and scarf. (c) Original sized probe image with occlusion.

The recognition accuracy of various comparing approaches on the AR dataset, wherein S1-G and S1-S represent images of sunglasses and images of scarf from Session 1 respectively, likewise S2-G and S2-S denote images from S2. Note that some of the comparing algorithms have more than one gallery image per subject, and the more gallery images per subject are used in experiment, the easier the recognition task would be. To compare with these methods, we also ran our RPSM with the same setting, i. e., 7 gallery images per identity. We indicate the number of gallery images per subject used by various algorithms in the column of #g. From the recognition result we can see that RPSM achieves superior performance over the other state-of-the-art methods on S1-G and S2-G, and obtains satisfactory results on S1-S and S2-S. The good performance of our approach can be credited to our subset matching scheme: the correspondence values of key points located among occlusion parts, such as sunglasses and scarf, were gradually set to zero during the matching process, hence outliers' impact on final distance metric were minimized. Only those matched key points in facial area were included into point set distance calculation. Another observation is RPSM performed consistently better than MLERPM in all four scenarios, validating the effectiveness of adding constraint to affine transformation matrix.

To further show the effectiveness of our algorithm, we recognized the identity from the original whole probe images without crop and alignment. That is the size of probe image will be 576 × 768 as in Fig. 13. In terms of gallery images, they were cropped 128×128 images. Hence, in this scenario, probe images were of different size from the gallery images and they were not aligned. Note that in this case, our RPSM approach performed the best throughout all four parts. One interesting phenomenon is that the recognition rates of MKD-SRC-GTP dropped a great deal in this scenario. The reason is that they used Harris-Laplacian detector as interest point detector, which is more sensitive to corner than to blob. Hence, when the hair regions were included in the probe images, a large portion of interest points were detected among the hair region (hairs appear like corners to feature detector). However, hairs across sessions are not as stable as facial features and they are not discriminative as well.
For EYB dataset, we randomly chose 32 images of each subject for training, and the remaining 32 for testing. In our experiments we synthesized contiguous-block-occluded images with occlusion levels ranging from 10% to 50%, by superimposing a correspondingly sized unrelated image randomly on each probe image, as in Fig. 5.8 We compared our algorithm with SRC and other three partial face recognition approaches, where we obtained some interesting results ,Before occlusion level arrived at 40%, our method performed better or comparably with SRC and MKD-SRC-GTP, but it degraded drastically when the occlusion percent reached more than 40%, while in the AR dataset, our method achieved quite satisfactory result where the percent of disguise for scarf is 40%. This is because in the experiment of AR dataset, disguise was either laid on the upper half or lower half of the face, discriminative features were almost half retained, while in this experiment, occlusion occurred randomly, emphieg. in Fig.5.8, when occlusion percent was 50%, most part of face area was occluded, making face match extremely difficult. Hence our method is suitable for scenarios where sufficient discriminative facial areas are available.

### E. Partial Face Recognition across Expression

We evaluated the robustness of our approach on partial face recognition with facial expressions on AR dataset. Specifically, for each person in AR, the neutral face in the first session was selected into the gallery images. Correspondingly, two smiling faces and two screaming faces from both sessions were chosen as the probe faces. These probe faces were further randomly transformed to simulate the partial face recognition across facial expression scenario. Some example faces are shown in Fig.5.9. records the recognition rates of the comparing approaches, where "S1-Sm" denotes the probe images which are smiling faces from Session 1 and "S2-Sc" the screaming faces from Session 2. It can be seen that recognizing identity from screaming faces is much more challenging than identifying from smiling ones. Among the comparing approaches, our RPSM consistently outperforms the others.

### F. Computational Time

Our RPSM matching procedure is implemented in MATLAB with a noncommercial solver, lpsolve which deploys the simplex methods. Having obtained the initial keypoint selection, our RPSM takes around 20 ms to match a pair of probe and gallery keypoints on a desktop with corei5 CPU @3.2GHZ, where the LP trust region shrinkage runs for 4-6 iterations. Note that the running time can be further shortened by implementing the method in C/C++.

## 3. Results

We have given a test image with blurred and we detect the original image successfully as shown I Fig. 3.


**Fig. 3**. Test image and detected image.

In another example we have given a test image with less clarity and we detected the original image as shown in fig. 4.


**Fig. 4**. Test image with low clarity and its detection.

In the below example we given test image with shaded eyes and we detected original image and shown in Fig. 5.

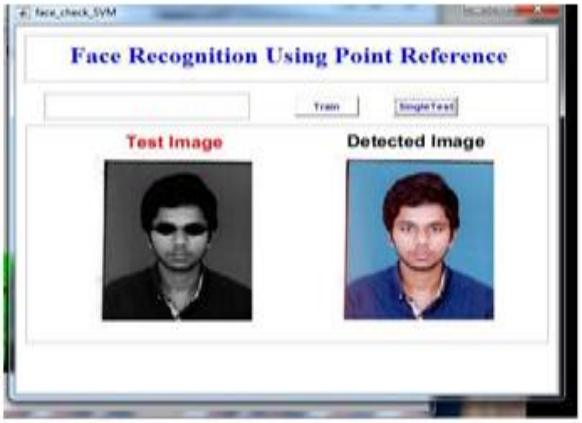


**Fig. 5.** Test image with shaded eyes and original image.

## Conclusion

Here we can recognize the faces clearly from the persons of interest from their partial faces. The proposed RPSM method is able to align the probe partial face to gallery facial images robustly even with the presence of occlusion, random partial crop, and exaggerated facial expressions. After face alignment, partial face recognition is achieved by measuring face similarity based on the proposed point set distance, which can be readily acquired with the face alignment result. The hallmark of the RPSM is its robust matching scheme, which considers both the geometric distribution consistency and the textural similarity. Moreover, constraint on the affine transformation is applied to prevent from unrealistic face warping. Experimental results on four widely used face datasets were presented to show the efficacy and limitations of our proposed method, the latter of which pointed out the direction for our future work.

## References

[1]. Partial face recognition by template matching 2015 International Conference on Emerging Research in Electronics, Computer Science and Technology (ICERECT).

[2]. N. Cuntoor, A. Kale, R. Chellappa, "Combining multiple evidences for gait recognition", *Proceedings of the international conference on acoustics speech and signal processing*, vol. 3, pp. 33-36, 2003.

[3]. Q. Zhao, D. Zhang, L. Zhang, N. Luo, "High resolution partial fingerprint alignment using pore-valley descriptors", *Pattern Recognition*, vol. 43, pp. 1050-1061, 2010

[4]. M. Marsico, M. Nappi, D. Riccio, "FARO: Face Recognition against Occlusions and Expression Variations", IEEE Transactions on System Man and Cybernetics-Part A: Systems and Humans, vol. 40, no. 1, pp. 121-132, 2010.

[5]. Partial face recognition: An alignment free approach IEEE Biometrics Compendium IEEE RFIC Virtual Journal, IEEE RFID Virtual Journal.

[6]. J. Wright, A. Y. Yang, A. Ganesh, S. S. Sastry, and Y. Ma.Robust face recognition via sparse representation. IEEE Transactions on Pattern Analysis and Machine Intelligence, 31:210-227, 2009.

[7]. A New Approach to Partial Face Recognition Amit V. Manapure (IJCSIT) International Journal of Computer Science and Information Technologies, Vol. 6 (1) , 2015, 52-56.

[8]. Shengcai Liao, Anil K. Jain, Fellow, IEEE, and Stan Z. Li "Partial Face Recognition:Alignment Free Approach" IEEE Transactions On Pattern Analysis And Machine Intelligence, Vol. 35, No. 5, May 2013.

[9]. Urk M A, Pentland A P. Face recognition using eigenfaces [C]. Computer Vision and Pattern Recognition, 1991.Proceedings CVPR'91.IEEE Computer Society Conference on. IEEE, 1991:586-591.

[10]. An efficient partial occluded face recognition system Neuro computing Volume 116, 20 September 2013, Pages,231-241.

[11]. V Sundara Siva Kumar Proceedings on NCOCS2K19 2019/09 Partial Face Recognition system. 10.13140/RG.2.2.35337.39526 section.

## About the Authors

Dr S Suryanarayana, is working as Professor & HOD in ECE department, MVSR Engineering College, Hyderabad, since June 2022. He completed his Post Graduation from Osmania University in 2002 and awarded PhD from JNTUH, Hyderabad in 2015. He has an overall teaching experience of 32 years. His interesting fields are Image processing, Neural Networks.
**ORCID ID: 0000-0001-6111-5010.**
**Researcher ID: HIR-1870-2022.**

Mr. V Sundara Siva Kumar, is working as an Assistant Professor in ECE department, MVSR Engineering College, Hyderabad, since November 2022 He completed his M.Tech in VLSI & ES. He has an overall teaching experience of 12 years. He is interested in Instrumentation Engineering and VLSI.
**ORCID ID: 0000-0003-3533-0125**.
**Researcher ID: AAC-1211-2019.**